ELSEVIER

International Journal of Solids and Structures 41 (2004) 4535–4550

INTERNATIONAL JOURNAL OF SOLIDS and STRUCTURES

www.elsevier.com/locate/ijsolstr

Antiplane stress analysis of an isotropic wedge with multiple cracks

R.T. Faal, A.R. Fotuhi, S.J. Fariborz *, H.R. Daghyani

Department of Mechanical Engineering, Amirkabir University of Technology Polytechnic Tehran, Hafez Avenue 424, Tehran 158754413, Iran

Received 17 September 2003; received in revised form 28 February 2004
Available online 26 April 2004

Abstract

Stress analysis is accomplished for an infinite isotropic wedge weakened by a screw dislocation. Two different cases of boundary conditions, i.e., traction–displacement and traction–traction, is considered for the wedge. The Mellin transform is utilized to solve the governing differential equation. The dislocation solution is employed for the analysis of wedges containing multiple cracks under antiplane deformation. The resultant system of singular integral equations is solved numerically to determine dislocation density on the cracks surfaces. This allows the calculation of crack opening displacements and stress intensity factors. The effects of wedge angle and cracks location and orientation on the stress intensity factors of straight cracks are investigated.

Keywords: Antiplane deformation; Multiple cracks; Screw dislocation; Stress intensity factor

1. Introduction

Stress analysis in a wedge weakened by dislocations is of some practical importance. The dislocation solution may serve as the Green's function for wedges containing multiple cracks and cavities with arbitrary orientations, locations, and configurations. The literature is replete with studies related to dislocations in different regions, e.g., Weertman (1996). For want of space, a few investigations focused on wedges with dislocations and/or cracks are mentioned below.

The stress field due to an edge dislocation located in a quarter plane is obtained by Keer et al. (1983). They also used the dislocation solution to analyze quarter planes weakened by a straight crack with various orientations. Hecker and Romanov (1992) treated the problem of edge dislocation in an infinite wedge. Stress arising along the interface between two dissimilar quarter planes induced by a dislocation situated on the interface or anywhere within the two quarter planes is obtained by Kelly et al. (1994). Wu (1998)

* Corresponding author. Tel.: +98-21-6454-3460; fax: +98-21-641-9736.
E-mail address: sjfariborz@yahoo.com (S.J. Fariborz).

0020-7683/$ - see front matter
doi:10.1016/j.ijsolstr.2004.03.005

derived the stress fields caused by a line force or dislocation in an infinite anisotropic wedge by employing the Mellin integral transform method. Kipinis (1979) analyzed the problem of an infinite elastic wedge bisected by a semi-infinite crack. The crack tip is located at a finite distance from the wedge vertex and the loading is a set of self-equilibrating moments and forces applied to the vertex. The solution of the problem is carried out via the Mellin transform and the Wiener–Hopf technique. This problem is reexamined by Sadykhov (1980) for a case where the self-equilibrating moments applied far from the wedge apex. The above-mentioned works dealt mainly with in-plane deformation of wedges with a dislocation. The problem of a dissimilar wedge containing a radial crack at the interface under antiplane deformation is solved by Erdogan and Gupta (1975). The method consists of the reduction of the related dual integral equations to a singular integral equation. The technique is applicable to wedges with several radial cracks aligned on the same direction. Another noteworthy contribution is the article by Ohr et al. (1985) wherein the complex potential technique was utilized to investigate the interaction of a semi-infinite wedge crack with a screw dislocation in an infinite domain.

The analysis of a screw dislocation in the wedge is accomplished in the first section of this paper. Two types of boundary conditions, i.e., displacement–traction and traction–traction for the wedge are considered. Equilibrium equation in terms of antiplane displacement component leads to the Laplace's equation. The Mellin transform is employed to obtain the solution. The behavior of displacement and stress fields in the vicinity of dislocation is studied which reveals the well-known Cauchy type singularity of stress components. The results of analysis are utilized to analyze wedges containing multiple cracks subjected to antiplane traction on the free edges. A system of singular integral equations is obtained for the dislocation density on the cracks surfaces. These equations are solved by the methodology developed by Erdogan et al. (1973). The technique allows the analysis of curved cracks with any smooth geometry. Moreover, cavities may be treated as closed cracks. For the latter configuration basically the same analysis prevails but the ensuing system of integral equations is not singular and requires a different numerical scheme for solution. The issue is beyond the scopes of the current study and will not be pursued further. In this article, however, numerical results for only multiple embedded straight cracks are presented. The influence of cracks orientation and location as well as wedge angle on the stress intensity factors is investigated through some numerical examples. For the particular case of wedge with a single radial crack the integral equation is identical with that of Erdogan and Gupta (1975) which confirms the validity of analysis.

2. Wedge with screw dislocation

The distributed dislocation technique is an efficient means for treating multiple curved cracks and cavities with smooth geometries. The major obstacle in the utilization of the method is the knowledge of stress fields due to a single dislocation in the region. This task for domains with wedge configuration containing a screw dislocation is taken up here. In the cylindrical coordinate system (R, θ, z), we consider an isotropic elastic wedge with infinite radius, and apex angle α which is infinitely extended in the z-direction. The only nonzero displacement component under antiplane deformation is the out of plane component $w(R, \theta)$. Consequently, the constitutive relationships in polar coordinates read as

$$\tau_{\theta z} = \frac{\mu}{R}\frac{\partial w}{\partial \theta}, \qquad \tau_{Rz} = \mu \frac{\partial w}{\partial R}, \tag{1}$$

where μ is the wedge elastic shear modulus. Utilizing (1) the equilibrium equation in terms of displacement may be written as

$$\Delta w(R, \theta) = 0, \tag{2}$$

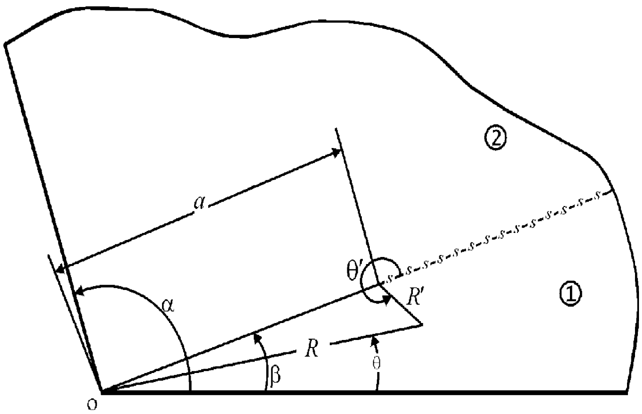

Fig. 1. Wedge weakened by a screw dislocation.

where Δ is the Laplace's operator. In order to situate a dislocation at the point (a, β), we divide the wedge into two regions $0 < \theta < \beta$ and $\beta < \theta < \alpha$ (Fig. 1). The conditions representing a Volterra type screw dislocation are (Barber, 1992),

$$\begin{aligned} w_1(r, \beta) - w_2(r, \beta) &= 0, \quad 0 < r < 1, \\ w_1(r, \beta) - w_2(r, \beta) &= \delta, \quad 1 < r < \infty, \end{aligned} \tag{3}$$

where $r = R/a$ is the dimensionless variable, subscripts 1 and 2 refer to the domain number, and δ designates the dislocation Burgers vector. The conditions of continuity and self-equilibrium of stress in the wedge containing dislocation imply that

$$\tau_{1\theta z}(r, \beta) = \tau_{2\theta z}(r, \beta). \tag{4}$$

The solution to (2) is accomplished by means of Mellin transformation. The Mellin transform for sufficiently regular function $f(r)$ is defined as

$$F(s) = \int_0^\infty f(r) r^{s-1} \, \mathrm{d}r, \tag{5}$$

where s is the complex variable. The inversion of Mellin transform yields

$$f(r) = \frac{1}{2\pi i} \int_{c-i\infty}^{c+i\infty} F(s) r^{-s} \, \mathrm{d}s. \tag{6}$$

The application of (5) to (2) leads to a second order ordinary differential equation, for each region. The solution to these equations is readily known

$$W_k(s, \theta) = a_k(s) \cos(\theta s) + b_k(s) \sin(\theta s), \quad k = 1, 2. \tag{7}$$

The Mellin transform of (3) and (4), provided that the Bromwich line in (6) is $c < 0$, results in

$$W_1(s, \beta) - W_2(s, \beta) = -\frac{\delta}{s}, \qquad \left.\frac{\partial W_1(s, \theta)}{\partial \theta}\right|_{\theta=\beta} = \left.\frac{\partial W_2(s, \theta)}{\partial \theta}\right|_{\theta=\beta}. \tag{8}$$

Depending upon the kind of boundary data on the edges of wedge, two different cases may be considered, i.e., displacement–traction and traction–traction conditions. These cases are analyzed separately in the following.

2.1. Displacement–traction

The wedge is considered to be fixed at the edge $\theta = 0$ and traction free at $\theta = \alpha$. Therefore, the boundary conditions became

$$w_1(r, 0) = 0, \qquad \tau_{2\theta z}(r, \alpha) = 0. \tag{9}$$

The above conditions by virtue of (1) and (5) reduce to

$$W_1(s, 0) = 0, \qquad \left.\frac{\partial W_2(s, \theta)}{\partial \theta}\right|_{\theta=\alpha} = 0. \tag{10}$$

Utilizing (8) and (10), the four unknown coefficients in (7) may be determined; and in view of (1) and (6) the stress components results in

$$\begin{aligned}
\tau_{\theta z} &= \mu\frac{\delta}{a}\frac{1}{2\pi i}\int_{c-i\infty}^{c+i\infty}\left[\frac{\sin((\alpha-\beta)s)\cos(\theta s)}{\cos(\alpha s)}\right]r^{-s-1}\,\mathrm{d}s, \quad 0\leqslant\theta\leqslant\beta,\\
\tau_{\theta z} &= -\mu\frac{\delta}{a}\frac{1}{2\pi i}\int_{c-i\infty}^{c+i\infty}\left[\frac{\cos(\beta s)\sin((\theta-\alpha)s)}{\cos(\alpha s)}\right]r^{-s-1}\,\mathrm{d}s, \quad \beta\leqslant\theta\leqslant\alpha,\\
\tau_{rz} &= -\mu\frac{\delta}{a}\frac{1}{2\pi i}\int_{c-i\infty}^{c+i\infty}\left[\frac{\sin((\alpha-\beta)s)\sin(\theta s)}{\cos(\alpha s)}\right]r^{-s-1}\,\mathrm{d}s, \quad 0\leqslant\theta\leqslant\beta,\\
\tau_{rz} &= -\mu\frac{\delta}{a}\frac{1}{2\pi i}\int_{c-i\infty}^{c+i\infty}\left[\frac{\cos(\beta s)\cos((\theta-\alpha)s)}{\cos(\alpha s)}\right]r^{-s-1}\,\mathrm{d}s, \quad \beta\leqslant\theta\leqslant\alpha.
\end{aligned} \tag{11}$$

The integrals in (11) can be evaluated employing contour integration and the residue theorem. The integrands are singular at points $s_i = (2i-1)\pi/(2\alpha)$, $i = 0, \pm 1, \pm 2, \ldots$ Considering the requirement imposed in the derivation of the first of (8) the Bromwich line in (11) should be chosen such that $-\pi/2\alpha < c < 0$. To carry out the contour integration, we require that the integrands in (11) vanish as $|s| \to \infty$. Consequently, for $0 < r \leqslant 1$, the contour of integration consists of the second and third quadrants of the complex S-plane, whereas for $1 \leqslant r < \infty$, the contour engulfs the first and fourth quadrants. Applying the residue theorem in the region $0 < r \leqslant 1$, we have

$$\begin{aligned}
\tau_{\theta z} &= \mu\frac{\delta}{\alpha a}\sum_{i=1}^{\infty}(-1)^i\sin\left(\frac{(2i-1)\pi(\alpha-\beta)}{2\alpha}\right)\cos\left(\frac{(2i-1)\pi\theta}{2\alpha}\right)r^{\frac{(2i-1)\pi}{2\alpha}-1}, \quad 0\leqslant\theta\leqslant\beta,\\
\tau_{\theta z} &= -\mu\frac{\delta}{\alpha a}\sum_{i=1}^{\infty}(-1)^i\cos\left(\frac{(2i-1)\pi\beta}{2\alpha}\right)\sin\left(\frac{(2i-1)\pi(\theta-\alpha)}{2\alpha}\right)r^{\frac{(2i-1)\pi}{2\alpha}-1}, \quad \beta\leqslant\theta\leqslant\alpha,\\
\tau_{rz} &= \mu\frac{\delta}{\alpha a}\sum_{i=1}^{\infty}(-1)^i\sin\left(\frac{(2i-1)\pi(\alpha-\beta)}{2\alpha}\right)\sin\left(\frac{(2i-1)\pi\theta}{2\alpha}\right)r^{\frac{(2i-1)\pi}{2\alpha}-1}, \quad 0\leqslant\theta\leqslant\beta,\\
\tau_{rz} &= \mu\frac{\delta}{\alpha a}\sum_{i=1}^{\infty}(-1)^i\cos\left(\frac{(2i-1)\pi\beta}{2\alpha}\right)\cos\left(\frac{(2i-1)\pi(\theta-\alpha)}{2\alpha}\right)r^{\frac{(2i-1)\pi}{2\alpha}-1}, \quad \beta\leqslant\theta\leqslant\alpha.
\end{aligned} \tag{12}$$

The stress components in the region $1 \leqslant r < \infty$ may be written by merely replacing π by $-\pi$, in the above equations. Utilizing equalities given in Appendix A, the stress components in the whole wedge region simplify to

$$\begin{aligned}\tau_{\theta z} &= \frac{\mu\delta}{2\alpha a} r^{\frac{\pi}{2\alpha}-1}\left(r^{\frac{\pi}{\alpha}}-1\right)\left[\frac{\cos\left(\frac{\pi(\theta+\beta)}{2\alpha}\right)}{1+r^{\frac{2\pi}{\alpha}}-2r^{\frac{\pi}{\alpha}}\cos\left(\frac{\pi(\theta+\beta)}{\alpha}\right)}+\frac{\cos\left(\frac{\pi(\theta-\beta)}{2\alpha}\right)}{1+r^{\frac{2\pi}{\alpha}}-2r^{\frac{\pi}{\alpha}}\cos\left(\frac{\pi(\theta-\beta)}{\alpha}\right)}\right]\\ \tau_{rz} &= -\frac{\mu\delta}{2\alpha a} r^{\frac{\pi}{2\alpha}-1}\left(r^{\frac{\pi}{\alpha}}+1\right)\left[\frac{\sin\left(\frac{\pi(\theta+\beta)}{2\alpha}\right)}{1+r^{\frac{2\pi}{\alpha}}-2r^{\frac{\pi}{\alpha}}\cos\left(\frac{\pi(\theta+\beta)}{\alpha}\right)}+\frac{\sin\left(\frac{\pi(\theta-\beta)}{2\alpha}\right)}{1+r^{\frac{2\pi}{\alpha}}-2r^{\frac{\pi}{\alpha}}\cos\left(\frac{\pi(\theta-\beta)}{\alpha}\right)}\right]\end{aligned} \tag{13}$$

The behavior of stress fields at the apex of wedge is identical with that obtained for isotropic finite wedges by Kargarnovin et al. (1997). To investigate the behavior of stress fields at the dislocation position we change the coordinate system according to Fig. 1. The relationships between the two coordinates may be written as

$$r^2 = 1 + r'^2 + 2r'\cos(\theta'), \quad \theta = \beta + \sin^{-1}\left[\frac{r'\sin\theta'}{\sqrt{1+r'^2+2r'\cos\theta'}}\right], \qquad 0 \leqslant \theta' \leqslant 2\pi, \tag{14}$$

where $r' = R'/a$. Substituting (14) into (13) and carrying out the necessary manipulation, it is easy to deduce that

$$(\tau_{\theta z}, \tau_{rz}) \sim \frac{1}{r'} \quad \text{as } r' \to 0. \tag{15}$$

It should be noted that the above Cauchy-type singularity is reported previously, e.g., Weertman and Weertman (1992), for a two-dimensional isotropic media containing a screw dislocation. The displacement fields are obtained by substituting stress component $\tau_{\theta z}$ from (13) into the first of (1), integrating the resultant expression with respect to θ and utilizing the first of boundary data (9). This leads to

$$w(r,\theta) = \frac{\delta}{2\pi}\left\{\tan^{-1}\left[\frac{2r^{\frac{\pi}{2\alpha}}}{r^{\frac{\pi}{\alpha}}-1}\sin\left(\frac{\pi}{2\alpha}(\theta+\beta)\right)\right]+\tan^{-1}\left[\frac{2r^{\frac{\pi}{2\alpha}}}{r^{\frac{\pi}{\alpha}}-1}\sin\left(\frac{\pi}{2\alpha}(\theta-\beta)\right)\right]\right\}. \tag{16}$$

Changing the coordinates in (16) according to (14) we may observe that the first term of (16) is single-valued function of variable θ' whereas the second term is multiple-valued. Selecting the proper branch of the second term on the cut surfaces as

$$\begin{aligned}&\lim_{\theta'\to 0}\tan^{-1}\left[\frac{2(1+r'^2+2r'\cos(\theta'))^{\frac{\pi}{4\alpha}}}{(1+r'^2+2r'\cos(\theta'))^{\frac{\pi}{2\alpha}}-1}\sin\left(\frac{\pi}{2\alpha}\sin^{-1}\left[\frac{r'\sin\theta'}{\sqrt{1+r'^2+2r'\cos\theta'}}\right]\right)\right]=0,\\ &\lim_{\theta'\to 2\pi}\tan^{-1}\left[\frac{2(1+r'^2+2r'\cos(\theta'))^{\frac{\pi}{4\alpha}}}{(1+r'^2+2r'\cos(\theta'))^{\frac{\pi}{2\alpha}}-1}\sin\left(\frac{\pi}{2\alpha}\sin^{-1}\left[\frac{r'\sin\theta'}{\sqrt{1+r'^2+2r'\cos\theta'}}\right]\right)\right]=2\pi,\end{aligned} \tag{17}$$

we conclude that (16) satisfies boundary condition (3).

2.2. Traction–traction

Suppose the wedge is traction free at the edges $\theta = 0$ and $\theta = \alpha$. The conditions imposed by a screw dislocation are given in (3) and the boundary conditions for the wedge read as

$$\tau_{1\theta z}(r,0) = 0, \qquad \tau_{2\theta z}(r,\alpha) = 0. \tag{18}$$

The above boundary data with the aid of the first (1) and transformation (5), yield

$$\left.\frac{\partial W_1(s,\theta)}{\partial\theta}\right|_{\theta=0} = 0, \qquad \left.\frac{\partial W_2(s,\theta)}{\partial\theta}\right|_{\theta=\alpha} = 0. \tag{19}$$

Utilizing (8) and (19) the coefficients in (7) may be computed. And an analysis analogous to case (a) results in

$$
\begin{aligned}
\tau_{\theta z} &= \mu\frac{\delta}{a}\frac{1}{2\pi i}\int_{c-i\infty}^{c+i\infty}\left[\frac{\sin((\alpha-\beta)s)\sin(\theta s)}{\sin(\alpha s)}\right]r^{-s-1}\,\mathrm{d}s, \quad 0\leqslant\theta\leqslant\beta,\\
\tau_{\theta z} &= -\mu\frac{\delta}{a}\frac{1}{2\pi i}\int_{c-i\infty}^{c+i\infty}\left[\frac{\sin(\beta s)\sin((\theta-\alpha)s)}{\sin(\alpha s)}\right]r^{-s-1}\,\mathrm{d}s, \quad \beta\leqslant\theta\leqslant\alpha,\\
\tau_{rz} &= \mu\frac{\delta}{a}\frac{1}{2\pi i}\int_{c-i\infty}^{c+i\infty}\left[\frac{\sin((\alpha-\beta)s)\cos(\theta s)}{\sin(\alpha s)}\right]r^{-s-1}\,\mathrm{d}s, \quad 0\leqslant\theta\leqslant\beta,\\
\tau_{rz} &= -\mu\frac{\delta}{a}\frac{1}{2\pi i}\int_{c-i\infty}^{c+i\infty}\left[\frac{\sin(\beta s)\cos((\theta-\alpha)s)}{\sin(\alpha s)}\right]r^{-s-1}\,\mathrm{d}s, \quad \beta\leqslant\theta\leqslant\alpha.
\end{aligned}
\tag{20}
$$

The singularities of (20) are located at $s_i = i\pi/\alpha$, $i=\pm 1,\pm 2,\ldots$ Carrying out the contour integration in the region $0<r\leqslant 1$, the stress components may be readily obtained

$$
\begin{aligned}
\tau_{\theta z} &= \mu\frac{\delta}{\alpha a}\sum_{i=1}^{\infty}(-1)^i\sin\left(\frac{i\pi(\alpha-\beta)}{\alpha}\right)\sin\left(\frac{i\pi\theta}{\alpha}\right)r^{\frac{i\pi}{\alpha}-1}, \quad 0\leqslant\theta\leqslant\beta,\\
\tau_{\theta z} &= -\mu\frac{\delta}{\alpha a}\sum_{i=1}^{\infty}(-1)^i\sin\left(\frac{i\pi\beta}{\alpha}\right)\sin\left(\frac{i\pi(\theta-\alpha)}{\alpha}\right)r^{\frac{i\pi}{\alpha}-1}, \quad \beta\leqslant\theta\leqslant\alpha,\\
\tau_{rz} &= -\mu\frac{\delta}{\alpha a}\sum_{i=1}^{\infty}(-1)^i\sin\left(\frac{i\pi(\alpha-\beta)}{\alpha}\right)\cos\left(\frac{i\pi\theta}{\alpha}\right)r^{\frac{i\pi}{\alpha}-1}, \quad 0\leqslant\theta\leqslant\beta,\\
\tau_{rz} &= \mu\frac{\delta}{\alpha a}\sum_{i=1}^{\infty}(-1)^i\sin\left(\frac{i\pi\beta}{\alpha}\right)\cos\left(\frac{i\pi(\theta-\alpha)}{\alpha}\right)r^{\frac{i\pi}{\alpha}-1}, \quad \beta\leqslant\theta\leqslant\alpha.
\end{aligned}
\tag{21}
$$

Carrying out some straightforward manipulations and using the relationships given in Appendix A the stress components in region $0<r\leqslant 1$, $0\leqslant\theta\leqslant\alpha$ may be recast to

$$
\begin{aligned}
\tau_{\theta z} &= \frac{\mu\delta}{2\alpha a}r^{\frac{\pi}{\alpha}-1}\left[\frac{r^{\frac{\pi}{\alpha}}-\cos\left(\frac{\pi(\theta-\beta)}{\alpha}\right)}{1+r^{\frac{2\pi}{\alpha}}-2r^{\frac{\pi}{\alpha}}\cos\left(\frac{\pi(\theta-\beta)}{\alpha}\right)}-\frac{r^{\frac{\pi}{\alpha}}-\cos\left(\frac{\pi(\theta+\beta)}{\alpha}\right)}{1+r^{\frac{2\pi}{\alpha}}-2r^{\frac{\pi}{\alpha}}\cos\left(\frac{\pi(\theta+\beta)}{\alpha}\right)}\right],\\
\tau_{rz} &= \frac{\mu\delta}{2\alpha a}r^{\frac{\pi}{\alpha}-1}\left[\frac{\sin\left(\frac{\pi(\theta+\beta)}{\alpha}\right)}{1+r^{\frac{2\pi}{\alpha}}-2r^{\frac{\pi}{\alpha}}\cos\left(\frac{\pi(\theta+\beta)}{\alpha}\right)}-\frac{\sin\left(\frac{\pi(\theta-\beta)}{\alpha}\right)}{1+r^{\frac{2\pi}{\alpha}}-2r^{\frac{\pi}{\alpha}}\cos\left(\frac{\pi(\theta-\beta)}{\alpha}\right)}\right].
\end{aligned}
\tag{22}
$$

The stress components in the region $1\leqslant r<\infty$, $0\leqslant\theta\leqslant\alpha$ may be obtained by replacing π by $-\pi$ and changing the sign of the relevant component in (22). Substituting the stress component $\tau_{\theta z}$ into the first of (1), integrating the resultant expression with respect to θ and ignoring the rigid body displacement, we arrive at the displacement field in the whole wedge region

$$
w(r,\theta)=\frac{\delta}{2\pi}\left\{\tan^{-1}\left[\frac{r^{\frac{\pi}{\alpha}}+1}{r^{\frac{\pi}{\alpha}}-1}\tan\left(\frac{\pi}{2\alpha}(\theta-\beta)\right)\right]-\tan^{-1}\left[\frac{r^{\frac{\pi}{\alpha}}+1}{r^{\frac{\pi}{\alpha}}-1}\tan\left(\frac{\pi}{2\alpha}(\theta+\beta)\right)\right]\right\}. \tag{23}
$$

An analysis identical to the displacement–traction case reveals that the first term of the displacement field (23) is multiple-valued on the dislocation line. Choosing the proper branch of the multiple-valued function leads to boundary data (3).

3. Isotropic wedge with arbitrary oriented cracks

The dislocation solutions accomplished in the preceding section may be employed to analyze wedges with several arbitrary curved cracks. For the sake of brevity of calculations we consider only straight cracks. Let N be the number of cracks extended from (a_i, γ_i) to (b_i, η_i), $i = 1, 2, \ldots, N$ in polar coordinates (Fig. 2). The antiplane traction on the surface of ith crack in terms of stress components in polar coordinates become

$$\tau_{\bar{\theta}z}(\rho_i, \theta_i) = \tau_{\theta z} \cos \varphi_i - \tau_{rz} \sin \varphi_i. \tag{24}$$

Suppose dislocations with unknown density $B_{zj}(\rho_j)$ are distributed on the infinitesimal segment $\rho_j < \rho < \rho_j + \mathrm{d}\rho_j$ at the surface of jth crack. The traction on the surface of ith crack due to the presence of above dislocation for displacement–traction case utilizing (13) and (24) becomes

$$\begin{aligned}\tau_{\bar{\theta}z}(\rho_i, \theta_i) = {} & \frac{\mu B_{zj}(\rho_j)}{2\alpha\rho_j} C_{ij}^{\frac{1}{2}-\frac{\alpha}{\pi}} \left[\frac{C_{ij} \cos\left(\frac{\pi(\theta_i+\theta_j)}{2\alpha} - \varphi_i\right) - \cos\left(\frac{\pi(\theta_i+\theta_j)}{2\alpha} + \varphi_i\right)}{1 + C_{ij}^2 - 2C_{ij} \cos\left(\frac{\pi(\theta_i+\theta_j)}{\alpha}\right)} \right. \\ & \left. + \frac{C_{ij} \cos\left(\frac{\pi(\theta_i-\theta_j)}{2\alpha} - \varphi_i\right) - \cos\left(\frac{\pi(\theta_i-\theta_j)}{2\alpha} + \varphi_i\right)}{1 + C_{ij}^2 - 2C_{ij} \cos\left(\frac{\pi(\theta_i-\theta_j)}{\alpha}\right)} \right] \left[(\mathrm{d}\rho_j)^2 + (\rho_j \mathrm{d}\theta_j)^2 \right]^{\frac{1}{2}}, \quad i \neq j,\end{aligned} \tag{25}$$

where $C_{ij} = (\rho_i/\rho_j)^{\pi/\alpha}$. Analogously from (24) and (22), the traction on the ith crack produced by the aforementioned distribution of dislocations for the traction–traction case is

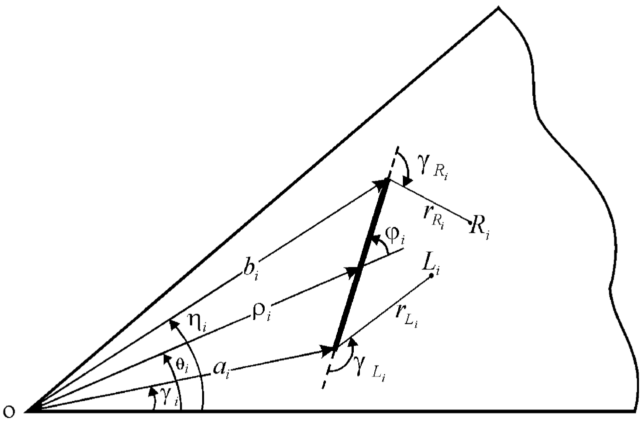

Fig. 2. Schematic view of a typical crack in a wedge.

$$\tau_{\bar\theta z}(\rho_i,\theta_i) = \frac{\mu B_{zj}(\rho_j)}{2\alpha\rho_j} C_{ij}^{1-\frac{\alpha}{\pi}} \left[\frac{C_{ij}\cos(\varphi_i) - \cos\left(\frac{\pi(\theta_i-\theta_j)}{\alpha} + \varphi_i\right)}{1 + C_{ij}^2 - 2C_{ij}\cos\left(\frac{\pi(\theta_i-\theta_j)}{\alpha}\right)} - \frac{C_{ij}\cos(\varphi_i) - \cos\left(\frac{\pi(\theta_i+\theta_j)}{\alpha} + \varphi_i\right)}{1 + C_{ij}^2 - 2C_{ij}\cos\left(\frac{\pi(\theta_i+\theta_j)}{\alpha}\right)} \right]$$
$$\times \left[(\mathrm{d}\rho_j)^2 + (\rho_j \mathrm{d}\theta_j)^2\right]^{\frac{1}{2}}, \quad a_i < \rho_i \leqslant \rho_j, \ \ i \neq j,$$
$$\tau_{\bar\theta z}(\rho_i,\theta_i) = -\frac{\mu B_{zj}(\rho_j)}{2\alpha\rho_j} C_{ij}^{-1-\frac{\alpha}{\pi}} \left[\frac{C_{ij}^{-1}\cos(\varphi_i) - \cos\left(\frac{-\pi(\theta_i-\theta_j)}{\alpha} + \varphi_i\right)}{1 + C_{ij}^{-2} - 2C_{ij}^{-1}\cos\left(\frac{\pi(\theta_i-\theta_j)}{\alpha}\right)} - \frac{C_{ij}^{-1}\cos(\varphi_i) - \cos\left(\frac{-\pi(\theta_i+\theta_j)}{\alpha} + \varphi_i\right)}{1 + C_{ij}^{-2} - 2C_{ij}^{-1}\cos\left(\frac{\pi(\theta_i+\theta_j)}{\alpha}\right)} \right]$$
$$\times \left[(\mathrm{d}\rho_j)^2 + (\rho_j \mathrm{d}\theta_j)^2\right]^{\frac{1}{2}}, \quad \rho_j \leqslant \rho_i < b_i, \ \ i \neq j. \tag{26}$$

Covering the cracks surfaces by dislocations, the principle of superposition may be invoked to obtain traction on the crack surfaces. The details of derivations are not given here but the following steps are taken. Eqs. (25) and (26) are integrated on the crack surfaces and the resultant tractions in each case are superimposed. The integration of (25) and (26) may be facilitated by describing cracks configurations in parametric form. The parameter $-1 \leqslant s \leqslant 1$ is chosen and the following change of variables is employed for straight cracks:

$$\begin{aligned}
\rho_i(s) &= \frac{1}{2}\left[a_i^2(1-s)^2 + b_i^2(1+s)^2 + 2(1-s^2)a_i b_i \cos(\eta_i - \gamma_i)\right]^{1/2}, \\
\theta_i(s) &= \gamma_i + \sin^{-1}\left[\frac{(s+1)b_i}{2\rho_i(s)}\sin(\eta_i - \gamma_i)\right], \\
\varphi_i(s) &= \gamma_i - \theta_i(s) + \sin^{-1}\left[\frac{b_i \sin(\eta_i - \gamma_i)}{\left[a_i^2 + b_i^2 - 2a_i b_i \cos(\eta_i - \gamma_i)\right]^{1/2}}\right].
\end{aligned} \tag{27}$$

The traction on the surface of ith crack yields

$$\tau_{\bar\theta zi}(\rho_i(s),\theta_i(s)) = \sum_{j=1}^{N} \int_{-1}^{1} b_{zj}(t) k_{ij}(s,t)\,\mathrm{d}t, \quad -1 \leqslant s \leqslant 1, \ \ i = 1,2,\ldots,N, \tag{28}$$

where $b_{zj}(t)$ is the dislocation density on the nondimensionalized length $-1 \leqslant t \leqslant 1$. The kernel $k_{ij}(s,t)$ in the displacement–traction case is

$$k_{ij}(s,t) = \left(\frac{\mu}{2\alpha}\right)\left[\left(\theta_j'(t)\right)^2 + \left(\frac{\rho_j'(t)}{\rho_j(t)}\right)^2\right]^{\frac{1}{2}}$$
$$\times (C_{ij}(s,t))^{\frac{1}{2}-\frac{\alpha}{\pi}} \left[\frac{C_{ij}(s,t)\cos\left(\frac{\pi(\theta_i(s)+\theta_j(t))}{2\alpha} - \varphi_i(s)\right) - \cos\left(\frac{\pi(\theta_i(s)+\theta_j(t))}{2\alpha} + \varphi_i(s)\right)}{1 + (C_{ij}(s,t))^2 - 2C_{ij}(s,t)\cos\left(\frac{\pi(\theta_i(s)+\theta_j(t))}{\alpha}\right)} \right.$$
$$\left. + \frac{C_{ij}(s,t)\cos\left(\frac{\pi(\theta_i(s)-\theta_j(t))}{2\alpha} - \varphi_i(s)\right) - \cos\left(\frac{\pi(\theta_i(s)-\theta_j(t))}{2\alpha} + \varphi_i(s)\right)}{1 + (C_{ij}(s,t))^2 - 2C_{ij}(s,t)\cos\left(\frac{\pi(\theta_i(s)-\theta_j(t))}{\alpha}\right)} \right], \quad i,j = 1,2,\ldots,N, \tag{29}$$

where $C_{ij}(s,t) = (\rho_i(s)/\rho_j(t))^{\pi/\alpha}$, θ_j and ρ_j are given in (27) and prime denotes differentiation with respect to the argument. Making use of (15) we may conclude that $k_{ij}(s,t)$ has Cauchy-type singularity for $i = j$ as $t \to s$. To illustrate this behavior the Hopital's rule is applied on (29) which leads to

$$k_{ii}(s,t)=\frac{a_{-1}}{s-t}+\sum_{m=0}^{\infty}a_m(s-t)^m \quad \text{as } t\to s, \tag{30}$$

where $a_{-1}=\mu/2\pi$. The coefficients a_m, $m=0,1,\ldots$ are regular functions of variable t in the interval $-1\leqslant t\leqslant 1$ which are lengthy and are not given here. The kernel of integral equation (28) for traction–traction case becomes

$$\begin{aligned}
k_{ij}(s,t)&=\left(\frac{\mu}{2\alpha}\right)\left[(\theta_j'(t))^2+\left(\frac{\rho_j'(t)}{\rho_j(t)}\right)^2\right]^{\frac{1}{2}}(C_{ij}(s,t))^{1-\frac{\alpha}{\pi}}\left[\frac{C_{ij}(s,t)\cos(\varphi_i(s))-\cos\left(\frac{\pi(\theta_i(s)-\theta_j(t))}{\alpha}+\varphi_i(s)\right)}{1+(C_{ij}(s,t))^2-2C_{ij}(s,t)\cos\left(\frac{\pi(\theta_i(s)-\theta_j(t))}{\alpha}\right)}\right.\\
&\quad\left.-\frac{C_{ij}(s,t)\cos(\varphi_i(s))-\cos\left(\frac{\pi(\theta_i(s)+\theta_j(t))}{\alpha}+\varphi_i(s)\right)}{1+(C_{ij}(s,t))^2-2C_{ij}(s,t)\cos\left(\frac{\pi(\theta_i(s)+\theta_j(t))}{\alpha}\right)}\right] \quad \text{for } 0<\rho_i(s)\leqslant\rho_j(t),\\
k_{ij}(s,t)&=\left(\frac{-\mu}{2\alpha}\right)\left[(\theta_j'(t))^2+\left(\frac{\rho_j'(t)}{\rho_j(t)}\right)^2\right]^{\frac{1}{2}}(C_{ij}(s,t))^{-1-\frac{\alpha}{\pi}}\left[\frac{(C_{ij}(s,t))^{-1}\cos(\varphi_i(s))-\cos\left(\frac{-\pi(\theta_i(s)-\theta_j(t))}{\alpha}+\varphi_i(s)\right)}{1+(C_{ij}(s,t))^{-2}-2(C_{ij}(s,t))^{-1}\cos\left(\frac{\pi(\theta_i(s)-\theta_j(t))}{\alpha}\right)}\right.\\
&\quad\left.-\frac{(C_{ij}(s,t))^{-1}\cos(\varphi_i(s))-\cos\left(\frac{-\pi(\theta_i(s)+\theta_j(t))}{\alpha}+\varphi_i(s)\right)}{1+(C_{ij}(s,t))^{-2}-2(C_{ij}(s,t))^{-1}\cos\left(\frac{\pi(\theta_i(s)+\theta_j(t))}{\alpha}\right)}\right] \quad \text{for } \rho_j(t)\leqslant\rho_i(s)<\infty,\\
&\quad i,j=1,2,\ldots,N.
\end{aligned} \tag{31}$$

Analogously, in the traction–traction case the kernel $k_{ij}(s,t)$ has Cauchy-type singularity for $i=j$ as $t\to s$ and the coefficient of singular term in (30) is $a_{-1}=(\mu/2\pi)\mathrm{sgn}(t-s)$, where sgn is the sign function. For the special case of a wedge with traction free edges, weakened by a single radial crack extended in $a\leqslant r\leqslant b$, and bisecting the wedge apex angle and under constant traction $\tau_{\bar{\theta}z}$ on the crack surface the integral equation (28) simplifies to

$$\tau_{\bar{\theta}z}(\rho(s))=\frac{\mu(b-a)}{2\alpha}\int_{-1}^{1}\frac{(\rho(s))^{\frac{\pi}{\alpha}-1}(\rho(t))^{\frac{\pi}{\alpha}}}{(\rho(s))^{\frac{2\pi}{\alpha}}-(\rho(t))^{\frac{2\pi}{\alpha}}}b_z(t)\,\mathrm{d}t, \tag{32}$$

where

$$\rho(s)=\frac{b+a}{2}+\frac{b-a}{2}s, \quad -1\leqslant s\leqslant 1. \tag{33}$$

The above integral equation is identical with that derived by Erdogan and Gupta (1975). This may validate the present analysis.

By virtue of Buckner's principle (Korsunsky and Hills, 1996) the left-hand side of Eq. (28) after changing the sign is the traction caused by the external loading on the uncracked wedge at the presumed surface of cracks. The applied traction on wedge with multiple cracks for displacement–traction case is known $\tau_{\theta z}(\rho,\alpha)=h(\rho)$. The stress components in the above wedge where cracks are removed are obtained by the direct application of Mellin transform. This results in

$$\tau_{\rho z}(\rho,\theta)=\frac{1}{\rho\alpha}\int_0^\infty \frac{b^{\frac{1}{2}}(1-b)\sin\left(\frac{\pi\theta}{2\alpha}\right)}{1+b^2+2b\cos\left(\frac{\pi\theta}{\alpha}\right)}h(\zeta)\,\mathrm{d}\zeta,$$
$$\tau_{\theta z}(\rho,\theta)=\frac{1}{\rho\alpha}\int_0^\infty \frac{b^{\frac{1}{2}}(1+b)\cos\left(\frac{\pi\theta}{2\alpha}\right)}{1+b^2+2b\cos\left(\frac{\pi\theta}{\alpha}\right)}h(\zeta)\,\mathrm{d}\zeta, \tag{34}$$

where $b=(\rho/\zeta)^{\pi/\alpha}$. The applied traction on the wedge with traction–traction boundary conditions is $\tau_{\theta z}(\rho,0)=\tau_{\theta z}(\rho,\alpha)=h(\rho)$. The stress fields in the uncracked wedge yield

$$\tau_{\rho z}(\rho,\theta)=\frac{2}{\rho\alpha}\int_0^\infty \frac{b(b^2-1)\cos\left(\frac{\pi\theta}{\alpha}\right)}{1+b^4-2b^2\cos\left(\frac{2\pi\theta}{\alpha}\right)}h(\zeta)\,\mathrm{d}\zeta,$$
$$\tau_{\theta z}(\rho,\theta)=\frac{2}{\rho\alpha}\int_0^\infty \frac{b(b^2+1)\sin\left(\frac{\pi\theta}{\alpha}\right)}{1+b^4-2b^2\cos\left(\frac{2\pi\theta}{\alpha}\right)}h(\zeta)\,\mathrm{d}\zeta. \tag{35}$$

We assume, without any loss of generality, that the applied traction on wedge is a patch load defined by

$$h(\rho)=\tau_0 H(l-\rho), \tag{36}$$

where l and τ_0 are constant length and traction, respectively, and $H(\rho)$ is the Heaviside-step function. Utilizing (24) and (34), the following traction should be applied on the surface of ith crack in displacement–traction case:

$$\tau_{\bar{\theta}zi}(\rho_i(s),\theta_i(s))=-\frac{\tau_0}{\rho_i(s)\alpha}\int_0^l \frac{b_i^{\frac{1}{2}}(s)\left[\cos\left(\frac{\pi\theta_i(s)}{2\alpha}+\varphi_i(s)\right)+b_i(s)\cos\left(\frac{\pi\theta_i(s)}{2\alpha}-\varphi_i(s)\right)\right]}{1+b_i^2(s)+2b_i(s)\cos\left(\frac{\pi\theta_i(s)}{\alpha}\right)}\mathrm{d}\zeta, \tag{37}$$

where $b_i(s)=(\rho_i(s)/\zeta)^{\pi/\alpha}$. Similarly for traction–traction case by virtue of (24) and (35) the left-hand side of (28) becomes

$$\tau_{\bar{\theta}zi}(\rho_i(s),\theta_i(s))=-\frac{2\tau_0}{\rho_i(s)\alpha}\int_0^l \frac{b_i(s)\left[\sin\left(\frac{\pi\theta_i(s)}{\alpha}+\varphi_i(s)\right)+b_i^2(s)\sin\left(\frac{\pi\theta_i(s)}{\alpha}-\varphi_i(s)\right)\right]}{1+b_i^4(s)-2b_i^2(s)\cos\left(\frac{2\pi\theta_i(s)}{\alpha}\right)}\mathrm{d}\zeta. \tag{38}$$

Employing the definition of dislocation density function, the equation for the crack opening displacement across the jth crack is

$$w_j^+(s)-w_j^-(s)=\int_{-1}^{s}\left[(\rho_j'(t))^2+(\rho_j(t)\theta_j'(t))^2\right]^{\frac{1}{2}}b_{zj}(t)\,\mathrm{d}t,\quad j=1,2,3,\ldots,N. \tag{39}$$

The displacement field is single-valued out of crack surfaces. Thus, the dislocation densities are subjected to the following closure requirement:

$$\int_{-1}^{1}\left[(\rho_j'(t))^2+(\rho_j(t)\theta_j'(t))^2\right]^{\frac{1}{2}}b_{zj}(t)\,\mathrm{d}t=0,\quad j=1,2,3,\ldots,N. \tag{40}$$

The Cauchy singular integral equations (28) and (40) are to be solved simultaneously, to obtain the dislocation density. This is accomplished by means of Gauss–Chebyshev quadrature scheme developed in Erdogan et al. (1973). The dislocation density is taken as

$$b_{zj}(t)=\frac{g_{zj}(t)}{\sqrt{1-t^2}},\quad -1<t<1,\ \ j=1,2,\ldots,N. \tag{41}$$

Substituting (41) into (28) and (40) and discretizing the domain, $-1<t<1$, the integral equations reduced to the following system of $N\times m$ linear algebraic equations:

$$\begin{bmatrix} A_{11} & A_{12} & A_{13} & \cdots & A_{1N} \\ A_{21} & A_{22} & A_{23} & \cdots & A_{2N} \\ A_{31} & A_{32} & A_{33} & \cdots & A_{3N} \\ \vdots & \vdots & \vdots & \ddots & \cdots \\ A_{N1} & A_{N2} & A_{N3} & \cdots & A_{NN} \end{bmatrix} \begin{bmatrix} g_{z1}(t_p) \\ g_{z2}(t_p) \\ g_{z3}(t_p) \\ \vdots \\ g_{zN}(t_p) \end{bmatrix} = \begin{bmatrix} q_1(s_r) \\ q_2(s_r) \\ q_3(s_r) \\ \vdots \\ q_N(s_r) \end{bmatrix}, \tag{42}$$

where the collocation points are

$$s_r = \cos\left(\frac{\pi r}{m}\right), \quad r = 1, \ldots, m-1, \qquad t_p = \cos\left(\frac{\pi(2p-1)}{2m}\right), \quad p = 1, \ldots, m. \tag{43}$$

The components of matrix and vectors in (42) are

$$A_{ij} = \frac{1}{m} \begin{bmatrix} k_{ij}(s_1, t_1) & k_{ij}(s_1, t_2) & \cdots & k_{ij}(s_1, t_m) \\ k_{ij}(s_2, t_1) & k_{ij}(s_2, t_2) & \cdots & k_{ij}(s_2, t_m) \\ \vdots & \vdots & & \vdots \\ k_{ij}(s_{m-1}, t_1) & k_{ij}(s_{m-1}, t_2) & \cdots & k_{ij}(s_{m-1}, t_m) \\ \pi\delta_{ij}\Delta_i(t_1) & \pi\delta_{ij}\Delta_i(t_2) & \cdots & \pi\delta_{ij}\Delta_i(t_m) \end{bmatrix},$$
$$g_{zj}(t_p) = [\, g_{zj}(t_1) \quad g_{zj}(t_2) \quad \cdots \quad g_{zj}(t_m) \,]^{\mathrm{T}},$$
$$q_j(s_r) = \frac{1}{\pi} [\, \tau_{\bar{\theta}zj}(\rho_j(s_1), \theta_j(s_1)) \quad \tau_{\bar{\theta}zj}(\rho_j(s_2), \theta_j(s_2)) \quad \cdots \quad \tau_{\bar{\theta}zj}(\rho_j(s_{m-1}), \theta_j(s_{m-1})) \quad 0 \,]^{\mathrm{T}}, \tag{44}$$

where δ_{ij} in the last row of A_{ij} is the Kronecker delta and superscript T stands for the transpose of a vector and $\Delta_i(t) = [(\rho_i'(t))^2 + (\rho_i(t)\theta_i'(t))^2]^{\frac{1}{2}}$.

The stress intensity factors for ith crack in terms of crack opening displacement (Fig. 2) is (Kanninen and Popelar, 1985)

$$k_{\mathrm{III}L_i} = \frac{\sqrt{2}}{4}\mu \lim_{r_{L_i}\to 0} \frac{w_i^-(s) - w_i^+(s)}{\sqrt{r_{L_i}}}, \qquad k_{\mathrm{III}R_i} = \frac{\sqrt{2}}{4}\mu \lim_{r_{R_i}\to 0} \frac{w_i^-(s) - w_i^+(s)}{\sqrt{r_{R_i}}}. \tag{45}$$

Setting the points L_i and R_i on the surface of the crack in the direction shown in Fig. 2, yields

$$\gamma_{L_i} = \pi, \qquad \gamma_{R_i} = \pi,$$
$$r_{L_i} = \left(\frac{1+s}{2}\right)[a_i^2 + b_i^2 - 2a_ib_i\cos(\eta_i - \gamma_i)]^{\frac{1}{2}}, \qquad r_{R_i} = \left(\frac{1-s}{2}\right)[a_i^2 + b_i^2 - 2a_ib_i\cos(\eta_i - \gamma_i)]^{\frac{1}{2}}. \tag{46}$$

The substitution of (41) into (39), and the resultant equation into (45) in conjunction with (46), leads to the stress intensity factors

$$k_{\mathrm{III}L_i} = -\frac{\sqrt{2}}{4}\mu[a_i^2 + b_i^2 - 2a_ib_i\cos(\eta_i - \gamma_i)]^{\frac{1}{4}} g_{zi}(-1),$$
$$k_{\mathrm{III}R_i} = \frac{\sqrt{2}}{4}\mu[a_i^2 + b_i^2 - 2a_ib_i\cos(\eta_i - \gamma_i)]^{\frac{1}{4}} g_{zi}(1). \tag{47}$$

The solutions of Eq. (42) are plugged into (47) to obtain the stress intensity factors.

4. Numerical examples and results

The analysis developed in the preceding section allows the consideration of a wedge with any number of cracks with different orientations. Validation of the numerical results is carried out by considering an isotropic half-plane containing a radial crack with changing orientation. The boundary of half-plane is traction free and a constant antiplane traction is applied on the crack surfaces. The dimensionless stress intensity factors determined by the present approach are in excellent agreement with the results in Tables 1 and 3 of the article by Erdogan and Gupta (1975).

In what follows, three numerical examples are presented to demonstrate the applicability of the outlined methodology. The applied traction in all examples is the patch load (36), with $l = 10$ cm. The first example is a wedge with apex angle $\alpha = 2\pi/3$ weakened by two equal-sized radial cracks bisecting the apex angle. The distance between the center of cracks are $l/5$ and the distance from the apex to the center of the first cracks is $l/10$, where l is the length of the patch load. Figs. 3 and 4, show the normalized stress intensity factors (SIF), k/k_0, where $k_0 = \tau_0\sqrt{a_0}$ is the SIF of the corresponding crack situated in an infinite plane under far field antiplane traction τ_0 and a_0 is half of the crack length, against the nondimensionalized crack lengths for the two different boundary conditions of wedge. As it may be observed, the SIF increases rapidly as the crack tip approaches the wedge apex. A similar trend may be noticed as the distance between the tips of cracks decreases. The formation of regions with high stress level is indeed attributed to the interaction of geometric singularities. Moreover, the slow growth of k_{R2}/k_0 versus the crack length may be noticed.

The effect of wedge angle on the SIF is examined by considering a radial crack with constant length $0.2l$, and distance from the center to the apex $c = 0.101l$. Figs. 5 and 6 display the normalized SIF verses the wedge angle for this crack with fixed orientation $\gamma = \pi/6$ as well as varying orientation wherein the crack constantly bisects the wedge angle. As the wedge angle increases the singularity of stress components at the

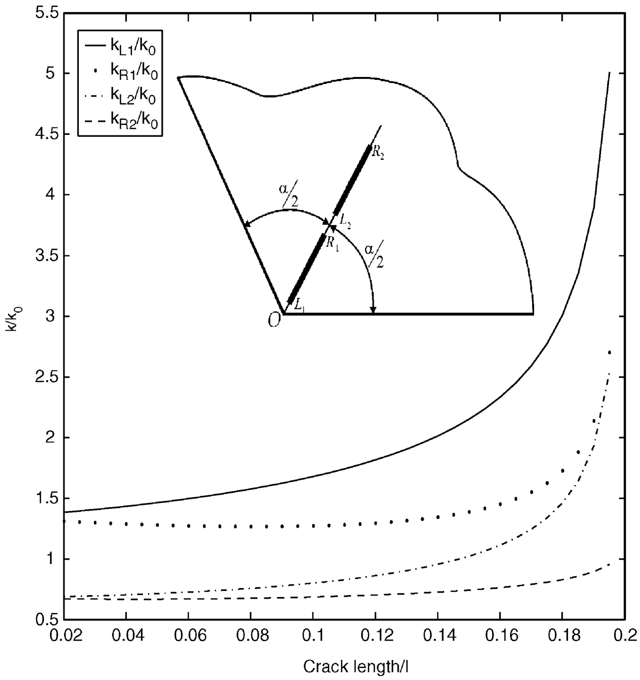

Fig. 3. Dimensionless stress intensity factors for two radial cracks with displacement–traction boundary condition.

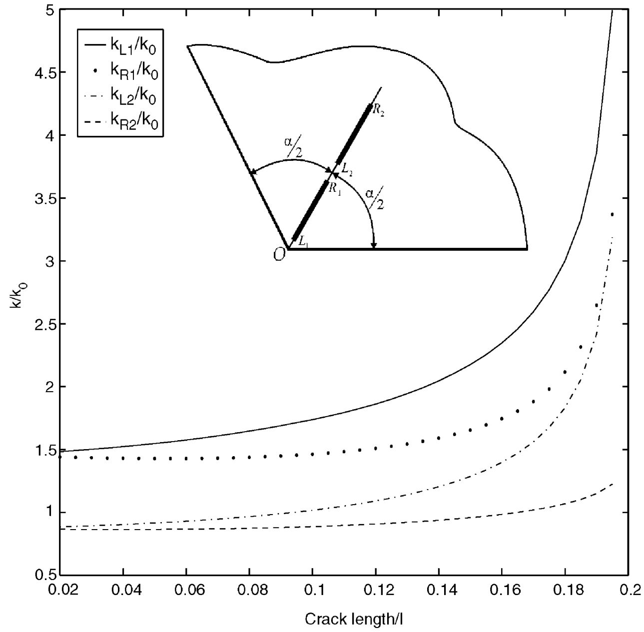

Fig. 4. Dimensionless stress intensity factors for two radial cracks with traction–traction boundary condition.

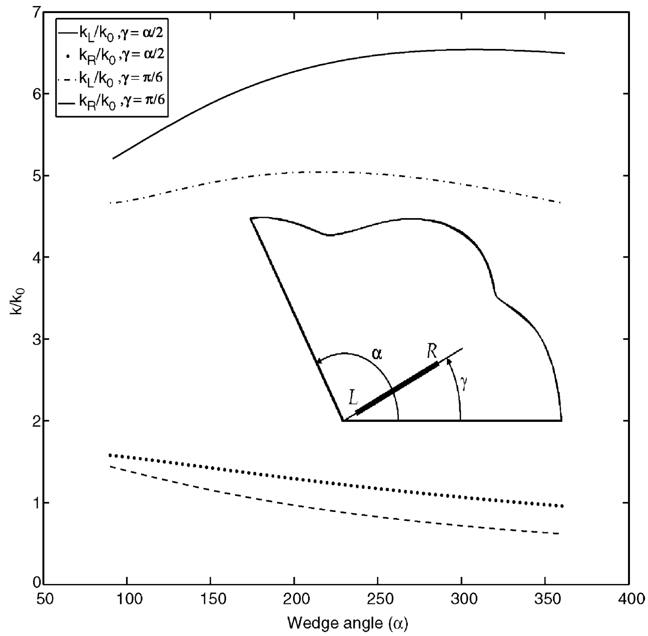

Fig. 5. Variations of k/k_0 with changing wedge apex angle and displacement–traction boundary condition.

wedge apex magnifies (Kargarnovin et al., 1997). On the contrary, according to Eqs. (37) and (38) the tractions on the crack surface diminish by increasing the wedge angle. The overall effects of the two parameters on the SIF are shown in the aforementioned two figures.

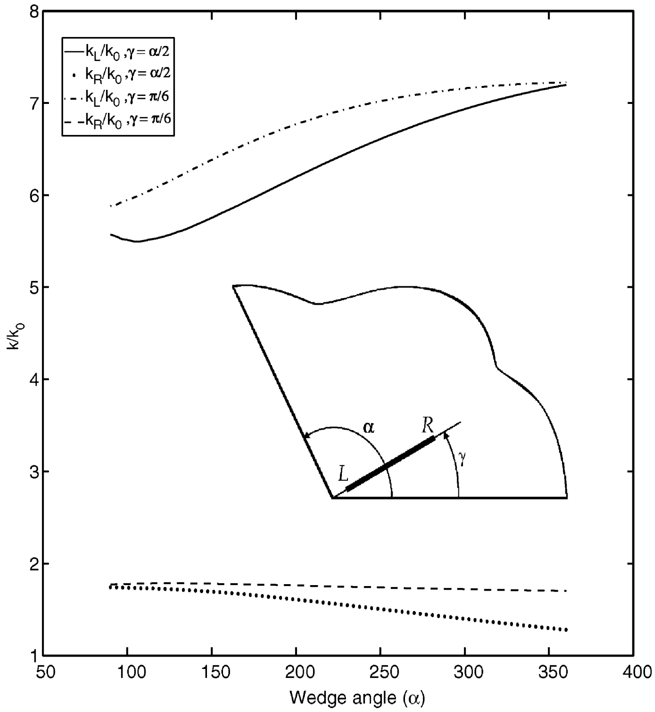

Fig. 6. Variations of k/k_0 with changing wedge apex angle and traction–traction boundary condition.

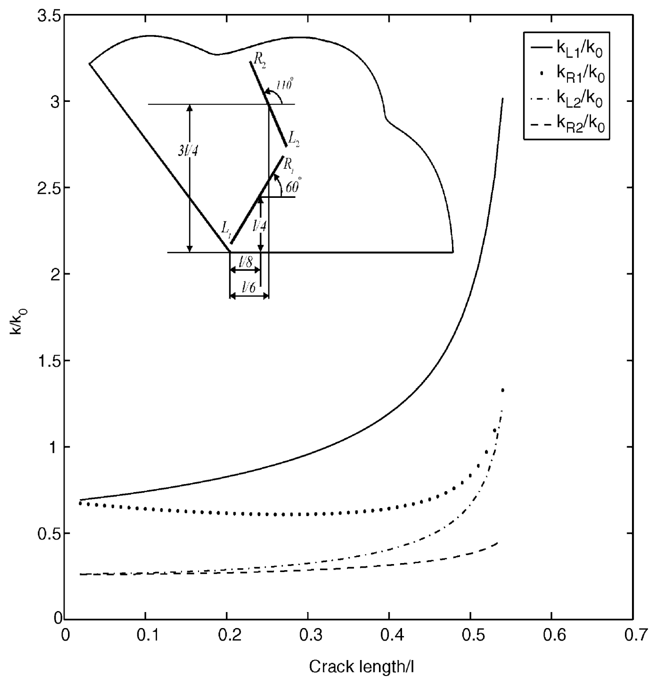

Fig. 7. Dimensionless stress intensity factors for two nonaligned cracks for displacement–traction boundary condition.

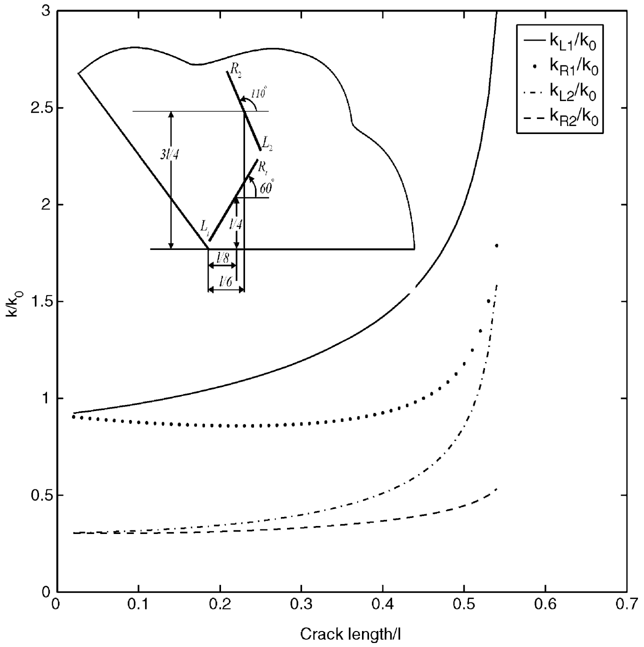

Fig. 8. Dimensionless stress intensity factors for two nonaligned cracks for traction–traction boundary condition.

In the last example, a wedge with angle $\alpha = 5\pi/6$ containing two cracks with equal lengths is considered. The variations of k/k_0 with nondimensionalized crack length are depicted in Figs. 7 and 8 for two different boundary conditions of the wedge. The crack closer to the wedge apex obviously experiences higher stress intensity factors.

5. Conclusion

A simple analysis is performed to obtain closed form expressions for displacement and stress fields due to the presence of a Volterra type screw dislocation in an elastic wedge. Two different types of boundary conditions are considered. The stress fields reveal Cauchy type singularity in the vicinity of dislocation. This is in agreement with the reported results in literature. The dislocation solutions are utilized to determine stress intensity factors for embedded straight cracks. The interaction of two adjacent cracks shows that the stress intensity factors of the two approaching crack tips intensify. Moreover, the stress intensity factor increases by increasing the crack length. The interaction between the wedge apex and crack tip is significant; the stress intensity factor grows rapidly as the distance between the crack tip and wedge apex reduces.

Appendix A

The following identities for $|K| \leqslant 1$ may be easily proved:

$$\sum_{i=1}^{\infty}(-K)^i \sin(ix) = -\frac{K\sin(x)}{1+K^2+2K\cos(x)},$$

$$\sum_{i=1}^{\infty}(-K)^i\cos(ix) = -K\frac{K+\cos(x)}{1+K^2+2K\cos(x)},$$

$$\sum_{i=1}^{\infty}(-K)^i\sin[(2i-1)x] = -\frac{K(1-K)\sin(x)}{1+K^2+2K\cos(2x)},$$

$$\sum_{i=1}^{\infty}(-K)^i\cos[(2i-1)x] = -\frac{K(K+1)\cos(x)}{1+K^2+2K\cos(2x)}.$$

In the case of $|K| > 1$, we should replace K by K^{-1}.

References

Barber, J.R., 1992. Elasticity. Kluwer Academic Publishers, Boston.

Erdogan, F., Gupta, G.D., 1975. Bounded wedge with an interface crack under antiplane shear loading. Int. J. Fract. 11 (4), 583–593.

Erdogan, F., Gupta, G.D., Cook, T.S., 1973. In: Sih, G.C. (Ed.), Numerical Solution of Integral Equations, Methods of Analysis and Solution of Crack Problems. Noordhoof, Leyden, Holland.

Hecker, M., Romanov, A.E., 1992. The stress fields of an edge dislocation near a wedge-shaped boundary. Phys. Stat. Sol. 130, 91–101.

Kanninen, M.F., Popelar, C.H., 1985. Advanced Fracture Mechanics. Oxford University Press, New York.

Kargarnovin, M.H., Shahani, A.R., Fariborz, S.J., 1997. Analysis of an isotropic finite wedge under antiplane deformation. Int. J. Solids Struct. 34 (1), 113–128.

Keer, L.M., Lee, J.C., Mura, T., 1983. Stress distributions for a quarter plane containing an arbitrarily oriented crack. J. Appl. Mech. 50, 43–49.

Kelly, P., Hills, D.A., Nowell, D., 1994. The complete stress field due to a dislocation located anywhere in two bonded quarter planes. J. Appl. Mech. 61, 992–993.

Kipinis, L.A., 1979. Elastic equilibrium of wedge with a crack. PMM 43 (1), 153–159.

Korsunsky, A.M., Hills, D.A., 1996. The solution of crack problems by using distributed strain nuclei. Proc. Instn. Mech. Eng. 210, 23–31.

Ohr, S.M., Chang, S.J., Thomson, R., 1985. Elastic interaction of a wedge crack with a screw dislocation. J. Appl. Phys. 57 (6), 1839–1843.

Sadykhov, A.E., 1980. Elasticity-theory problem for wedge with semi-infinite crack subjected to point moment. Sov. Appl. Mech. 16 (5), 431–437.

Weertman, J., 1996. Dislocation Based Fracture Mechanics. World Scientific Publishing Co, Singapore.

Weertman, J., Weertman, J.R., 1992. Elementary Dislocation Theory. Oxford University Press, New York.

Wu, K.C., 1998. The elastic fields of a line force or dislocation in an isotropic wedge. Int. J. Solids Struct. 35 (26–27), 3483–3495.